Dlk1/Pref-1 exhibits a distinct vascular role as a strong inhibitor of angiogenesis

Patricia Rodríguez[1]†, Maria Angeles Higueras[1]†, Alvaro González-Rajal[2], Arantxa Alfranca[3], Rosa Ana García-Fernández[4], María Monsalve[5], Fernando Rodríguez-Pascual[1], Juan Miguel Redondo[3], Jose Luis de la Pompa[2], Jorge Laborda[6] and Santiago Lamas[1]*

Subheading: Dlk1 as an angiogenesis inhibitor

One-sentence summary: Dlk1/Pref-1 is expressed in adult endothelial cells and is able to inhibit angiogenesis both in vitro and in vivo, an effect also conserved in model organisms as zebrafish.

1 Laboratorio Mixto CSIC-FRIAT, Centro de Biología Molecular "Severo Ochoa", Madrid, Spain

2 Departamento de Biología del Desarrollo Cardiovascular, Centro Nacional de Investigaciones Cardiovasculares (CNIC), Madrid, Spain

3 Departamento de Biología Vascular e Inflamación, CNIC, Madrid, Spain

4 Departamento de Anatomía Patológica, Facultad de Veterinaria, Universidad Complutense, Madrid, Spain

5 Departamento de Cardiología Regenerativa, CNIC, Madrid, Spain

6 Departamento de Bioquímica, Universidad de Castilla-La Mancha, Albacete, Spain

† Contributed equally

* To whom correspondence should be addressed. E-mail:slamas@cbm.uam.es

The protein Dlk1/Pref-1 is highly expressed in pre-adipocytes where it contributes to inhibit their differentiation into adipocytes and adipogenesis. We herein report its presence in adult vascular endothelial cells of different species at moderate but detectable levels. Dlk1 overexpression strongly inhibited basal and VEGF-induced formation of angiotubes while lung endothelial cells from Dlk1 null mice were highly angiogenic. In vivo studies demonstrated the capacity of Dlk1 to inhibit neovessel formation in subcutaneous matrigel plugs and an altered pattern of angiogenesis in retinas from null mice. This phenotype was accompanied by an increased number of filopodia and tip cells in the affected regions. In zebrafish embryos the expression of human Dlk1 promoted a disturbed pattern of intersegmental vascularization while the knockdown of the homologous protein was associated with ectopic angiogenesis. Our results unveil a novel role for Dlk1 in the regulation of angiogenesis and set the basis for investigating its action in pathological settings.

Dlk1/Pref-1 is a transmembrane protein pertaining to the epidermal growth factor superfamily and initially described in neuroendocrine tumors and preadipocytes (*1, 2*) While it has been described that Dlk1 may act as a powerful inhibitor of adipogenesis (*3*), several reports support that it may operate as a non canonical ligand of the Notch pathway, as it lacks the DSL domain conserved in classic Notch ligands mediating ligand-receptor interaction (*4-6*). This structural feature has been related to its capacity to inhibit Notch signaling in different cellular systems and organisms, by the interaction with specific EGF-like repeats and with potentially diverse effects on adipogenesis depending on the cell context and state of Notch activation (*7*). Since the Notch signaling pathway is essential for vascular development and physiology by controlling angiogenesis in pre and postnatal life (*8, 9*), we reasoned that Dlk1 could contribute to regulate this process in adult endothelial cells. Angiogenesis, defined as the formation of new blood vessels from pre-existing ones, is a central process in embryonic and postnatal life and the object of intense study as an area for tumor therapy (*10*).

Given the scarce information on Dlk1 in the vasculature, we first studied its expression in several endothelial cell types and species. Dlk1 was expressed in murine, human, porcine and bovine adult endothelial cells, although at moderate levels compared to pre-adipocytes (fig. S1 and Table 1). We then tested the capacity of Dlk1 to regulate the formation of angiogenic tube-like structures (angiotubes) in endothelial cells and found that overexpressed Dlk1 significantly abrogated the number of angiotubes both in the presence and absence of VEGF (fig.S2). Consistently, murine lung endothelial cells (MLEC) derived from Dlk1 null mice (*11*) showed increased formation of angiotubes with independence of VEGF presence (fig. 1A). This phenotype was reversed by the introduction of adenoviral constructs bearing Dlk1 (fig.1B). In addition, endothelial cells overexpressing Dlk1 exhibited a retarded ability of re-endothelization after 18 hours of in-plate endothelial wounding (scratch assay) (fig. S3A,C). In contrast, wound closure was significantly accelerated in MLEC from Dlk1 null mice (fig.S3B,C and supplementary video 1). As these assays do not clearly discern the differential contribution of migration and proliferation to the final effect observed, we evaluated the effect of Dlk1 suppression on endothelial cell viability and proliferation and found that the absence of Dlk1 significantly correlated with increased cell viability and proliferation (fig.S4), thus pointing to a mixed inhibitory effect on migration and proliferation of Dlk1 in these endothelial cell types.

To examine the effect of Dlk1 on angiogenesis in an ex-vivo model we studied the outgrowth of endothelial cells from aortic explants obtained from WT or Dlk1 null mice. Aortic segments from null mice exhibited a significantly higher pro-angiogenic profile (fig. 2A) which was abrogated in a dose-dependent fashion when Dlk1 was expressed in aorta explants of the null background (fig.2B). We then investigated the effect of adenoviral constructs for Dlk1 in a vivo model of ectopic angiogenesis based on the formation of vessels in Matrigel® plugs implanted subcutaneously in the abdominal region of healthy mice. Whereas VEGF-treated plugs showed macroscopic neovessel formation and increased hemoglobin content, these were drastically reduced in plugs exposed to adenoviral constructs of Dlk1compared to controls, an effect comparable in magnitude to that observed in plugs treated with the γ-secretase inhibitor DAPT (fig. 3A,B). Plugs bearing Dlk1 or DAPT showed significantly reduced number of vascular structures (fig. 3B).

In order to confirm the antiangiogenic role of Dlk1 in vivo we next studied the potential differences in the formation of retinal vessels of Dlk1 null mice compared to their wild-type counterparts. Retinas from null mice showed regions of hypervascularization at p5 and p14 (fig.4A and fig.S5). In the developing murine retina sprouting angiogenesis correlates well with the formation of endothelial tip cells and filopodia (*8*). A detailed study of the affected regions in the retinas of Dlk1 null mice demonstrated an increase in the number of filopodia and tip cells (fig.4B), in consistence with an underlying active dysregulated pro-angiogenic program. Overall, our results support that Dlk1 acts as a brake for proliferation, migration and angiogenesis in the vascular endothelium of post-natal mammals.

In order to investigate if the role of Dlk1 in angiogenesis could be generalized to other vertebrate models, we performed experiments in embryos from *Danio Rerio* (zebrafish), in which the human version of Dlk1 was overexpressed by egg injection at the time of fertilization. Three days after the injection, embryos expressing Dlk1 showed a dose-dependent abnormal pattern of dorsal vascularization, manifested in aberrant intersegmental branching and lack of a established dorsal longitudinal anastomotic vessel (fig.5, panels F,I, M). To decipher if the Dlk1 had a role by itself in the development of zebrafish vasculature, the endogenous homologous mRNA was targeted with a morpholino. At six days post fertilization the larvae showed ectopic subintestinal angiogenesis (fig.5, panel K) which followed a dose-dependent effect (fig.5, panel N). This phenotype was rescued by the concomitant expression of human Dlk1 (fig.5, panel L). Our results suggest that Dlk1 plays a role in the developing vasculature of zebrafish, hence supporting that this protein contributes to rein in the general angiogenic program.

Several reports lend a basis for the interaction between Dlk1 and the Notch signaling pathway suggesting that the former exerts an antagonistic role due to its capacity to bind EGF-like repeats, as shown in vitro for Notch 1 (*4*, *7*). However, other authors have proposed alternative modes of action for Dlk1 invoking direct interaction with fibronectin (*12*). We addressed the potential interaction of Dlk1 with the Notch signaling pathway by using several approaches. First, we found that the expression of the Notch-dependent luciferase reporter Hes-1, was reduced in a dose-dependent manner in endothelial cells expressing Dlk1 (fig.S6A), at levels comparable to the effects observed with the γ-secretase inhibitor DAPT (fig.S6B). We then studied the

abundance of Notch signaling pathway related proteins in MLEC from Dlk1 null mice and observed that the levels of the Notch intracellular domain (NICD) and the downstream transcriptional effector Hey1 were markedly augmented (fig.S7A). As Notch receptors promote signaling through the family of Snail proteins we studied their presence in endothelial cells from null mice, consistently observing increased levels of Snail and Slug compared to MLEC from wild-type mice (fig. S7B). Increasing concentrations of NICD promoted correlative changes in angiotube formation and associated Hes-1 activity, which was inhibited by DAPT (fig.S8). In keeping with previous reports (*13*), PAEC stably expressing NICD showed high levels of Hes-1-dependent luciferase expression. Of interest, angiotube formation in these cells was not reduced in the presence of Dlk1 (fig.S9), thus suggesting that the interaction between Dlk1 and the Notch receptor occurs at a proximal step which prevents it from regulating angiogenesis once the Notch-dependent signal is established (fig.S9). Finally, studies in zebrafish embryos showed that silencing of Dlk1 in the zebrafish was associated to increased expression of the Notch-dependent effector Rbp, whereas injection of embryos with the human Dlk1 protein reversed this effect (fig.S10). Taken together, these data strongly support that Dlk1 inhibits the Notch signaling pathway, and that this inhibition results in a profound alteration of angiogenesis in the different models evaluated.

The molecular level of interaction between Dlk1 and the Notch pathway germane to the regulation of postnatal angiogenesis remains to be defined. It has been established that three of the five canonical Notch ligands (Jagged 1, Dll1 and Dll4) are expressed in endothelial cells and play critical roles in vascular angiogenesis (*8*). For example, maintenance of arterial identity relies on the Notch 1-Dll1 interaction (*14*). In zebrafish, the absence of Notch promotes a shift towards the tip cell behavior, favoring sprouting (*15*). Heterozygous deletion of Dll4 or pharmacological inhibition of Notch signaling was associated with increased numbers of filopodia-extending endothelial tip cells and increased expression of tip cell marker genes compared with controls (*16*), thus suggesting that Dll4 is a negative regulator of vascular sprouting. Dll4 and Jagged 1 have opposing effects on sprouting angiogenesis mediated by VEGF signaling, by controlling the equilibrium between tip and stalk cells through a mechanism regulated by the glycosyltransferase Fringe, which post-translationally modifies the Notch receptors (*17*). The phenotype found in the retinas of null Dlk1 mice (increased number

of vessels, tip cells and filopodia in selective areas) is consistent with the antiangiogenic action of Dlk1 observed in cells and in the zebrafish model. However, given that Dlk1 is interfering with Notch signaling, a clear interpretation of this phenotype in the light of previously reported defects in retinal vasculature of mice where canonical ligands of the Notch pathway had been genetically modified, is not obvious. The interaction between canonical and non canonical Notch ligands is a complex one (*18*) and further studies are needed to establish the level of interaction of Dlk1 with the canonical ligands in the vasculature.

The regulation of angiogenesis in tumors is object of intense study in the context of providing an effective means of deferring or suppressing tumoral growth. However, tumors seem to find mechanisms of escape from anti VEGF-directed therapies (*19*) and hence it is essential to search for new candidates and targets mediating an antiangiogenic effect. In this pathological setting, and given the independence of Dlk1 from VEGF to inhibit angiogenesis, it will be worth determining the potential of Dlk1 to abrogate tumor-dependent angiogenesis.

Figure Legends

Fig. 1. Lung endothelial cell tube formation is enhanced in Dlk1 null mice. (**A**) Representative images from wild-type and Dlk1 null isolated cells in the presence or not of VEGF. Quantitative analysis represents number of tube-like structures from three independent preparations per group. Values are presented as mean $\pm$ SEM assayed per duplicate (*$p<0.05$). (**B**) Endothelial cells from Dlk1 null mice were infected with adenoviruses GFP or Dlk1-GFP; inhibition of angiogenesis is present in Dlk1 null cells transducing Dlk1.

Fig. 2. Sprouting angiogenesis is enhanced in aorta explants from Dlk1 null mice. (**A**) Representative images from wild-type and Dlk1 null aorta segments. The quantification of lengths from vessel-like structures (lower panel) shows an increase in KO neovessel outgrowth of null mice. Values are presented as mean $\pm$ SEM of n=35 aortic rings from six mice; *$p<0.05$. (**B**) The pro-angiogenic response of the null mice is abolished in explants pre-incubated with a Dlk1 adenovirus (Ad.Dlk1-GFP) in a concentration-

dependent manner, $1x10^9$ (middle panel) and $5x10^9$ (lower panel) plaque-forming units/mL compared to Ad.GFP (upper panel).

Fig. 3. Dlk1 inhibits angiogenesis in vivo. Ectopic angiogenesis was analyzed in Matrigel plugs containing adenovirus control, Ad.GFP, or plugs containing VEGF plus adenovirus control, VEGF plus adenovirus Dlk1, VEGF plus adenovirus Dlk1-GFP, VEGF plus DAPT and VEGF plus vehicle, DMSO. (**A**) Photograph of plugs with the different experimental conditions after 10 days of implantation. The quantification of hemoglobin content (right panel) shows that the VEGF pro-angiogenic effect is abolished in plugs containing Dlk1 or DAPT. Values represent mean ± SEM from six mice. ($p<0.05$ vs Ad.GFP plus VEGF). (**B**) Hematoxilin and eosin-stained sections of the plugs shows decreased vascularization in Ad.Dlk1, Ad.Dlk1-GFP and DAPT-treated plugs. Scale bars, 30 μm. (**C**) CD31 staining

Fig. 4. Altered retinal angiogenesis in Dlk1 null mice. (**A**) Confocal images of retinas from wild–type or Dlk1 null mice p5 and p14 pups stained for isolectin B4. Retinas of null mice p5 show a hyperfused plexus compared to wild-type. Right panel depicts the quantification of retinal areas covered by vessels. Bars represent mean ± SEM from ten mice. (*$p<0.05$). (**B**) Isolectin B4 immunofluorescence showing increased tip cell and filopodia in the Dlk1 null p5 pups angiogenic front. Squared areas are blown-up in the right panels. Bar graph depicts the quantitative analysis of tip cells and filopodia in wild-type and null pups (*$p<0.05$).

Fig. 5. Effects of Dlk1 on angiogenesis and circulation in zebrafish. Tg(Fli:eGFP) embryos at 72 h post fertilization (**A-I**) and at day 6 post fertilization (**J-L**). (**A,B,D,E,G,H**) Bright-field images. (**C,F,I,J,K,L**) Confocal microscopy images. General morphology (**A,B**) and intersegmental artery sprouts and GATA-dsRED-labeled erythrocytes (**C**) from a wild-type embryo injected with 500 ng of control cDNA plasmid. (**D-I**) Embryos injected with 500 ng of Dlk1 cDNA. Note the aberrant sprouting of the intersegmental vessel (ISV) and the lack of normal blood flow. This phenotype is more dramatic on (**G**,**H,I**). (**J**) Embryo injected with 250 μM control morpholino oligonucleotide. (**K**) Ectopic sprouts of the sub-intestinal vessels (SIV) in a

Dlk1-deficient embryo. (**L**) Phenotype after co-injection of Dlk1 morpholino and Dlk1 cDNA. (**M**) Quantification of ISV defects in 72 hpf embryos injected with Dlk1 cDNA at different concentrations. (**N**) Quantification of ectopic angiogenesis in day 6 pf larvae injected with control morpholino, Dlk1 morpholino alone or Dlk1 morpholino co-injected with Dlk1 cDNA.

REFERENCES

1. J. Laborda, E. A. Sausville, T. Hoffman, V. Notario, *J Biol Chem* **268**, 3817 (1993).
2. C. M. Smas, H. S. Sul, *Cell* **73**, 725 (1993).
3. H. S. Sul, *Mol Endocrinol* **23**, 1717 (2009).
4. V. Baladron *et al.*, *Exp Cell Res* **303**, 343 (2005).
5. M. L. Nueda, J. J. Garcia-Ramirez, J. Laborda, V. Baladron, *J Mol Biol* **379**, 428 (2008).
6. S. J. Bray, S. Takada, E. Harrison, S. C. Shen, A. C. Ferguson-Smith, *BMC Dev Biol* **8**, 11 (2008).
7. M. L. Nueda, V. Baladron, B. Sanchez-Solana, M. A. Ballesteros, J. Laborda, *J Mol Biol* **367**, 1281 (2007).
8. T. Gridley, *Curr Top Dev Biol* **92**, 277 (2010)
9. K. Takeshita *et al.*, *Circ Res* **100**, 70 (2007).
10. R. S. Kerbel, *N Engl J Med* **358**, 2039 (2008).
11. R. Raghunandan *et al.*, *Stem Cells Dev* **17**, 495 (2008).
12. Y. Wang, L. Zhao, C. Smas, H. S. Sul, *Mol Cell Biol* **30**, 3480 (2010).
13. L. A. Timmerman *et al.*, *Genes Dev* **18**, 99 (2004).
14. I. Sorensen, R. H. Adams, A. Gossler, *Blood* **113**, 5680 (2009).
15. A. F. Siekmann, N. D. Lawson, *Nature* **445**, 781 (2007).
16. S. Suchting *et al.*, *Proc Natl Acad Sci U S A* **104**, 3225 (2007).
17. R. Benedito *et al.*, *Cell* **137**, 1124 (2009).
18. B. D'Souza, A. Miyamoto, G. Weinmaster, *Oncogene* **27**, 5148 (Sep 1, 2008).
19. G. Bergers, D. Hanahan, *Nat Rev Cancer* **8**, 592 (2008).

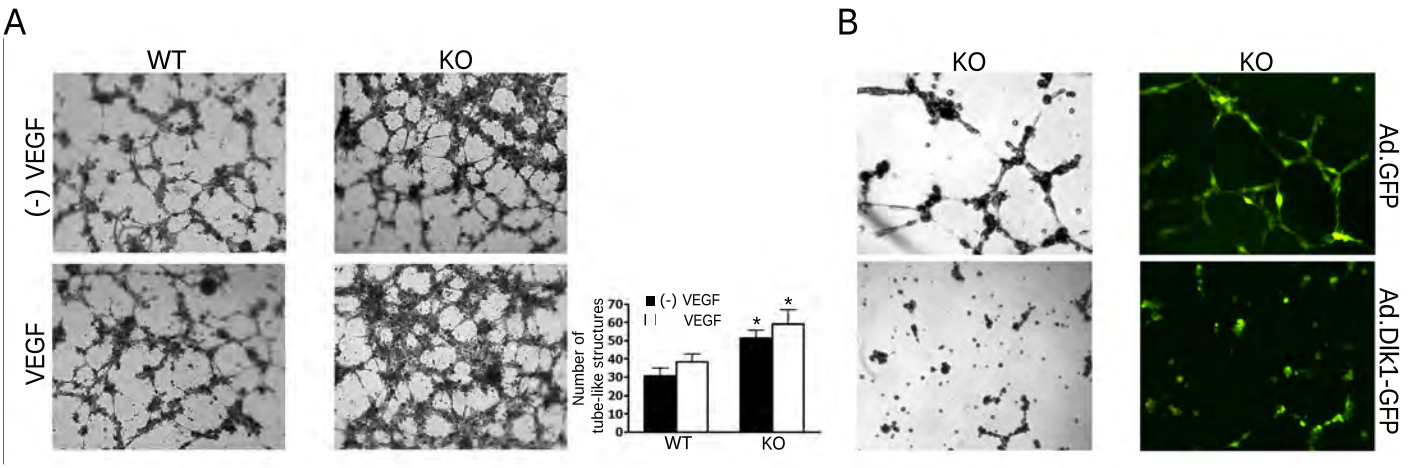
A
WT
KO
(-) VEGF
VEGF
Number of tube-like structures
(-) VEGF
VEGF
70
60
50
40
30
20
10
0
*
*
WT
KO
B
KO
KO
Ad.GFP
Ad.Dlk1-GFP

Fig 1

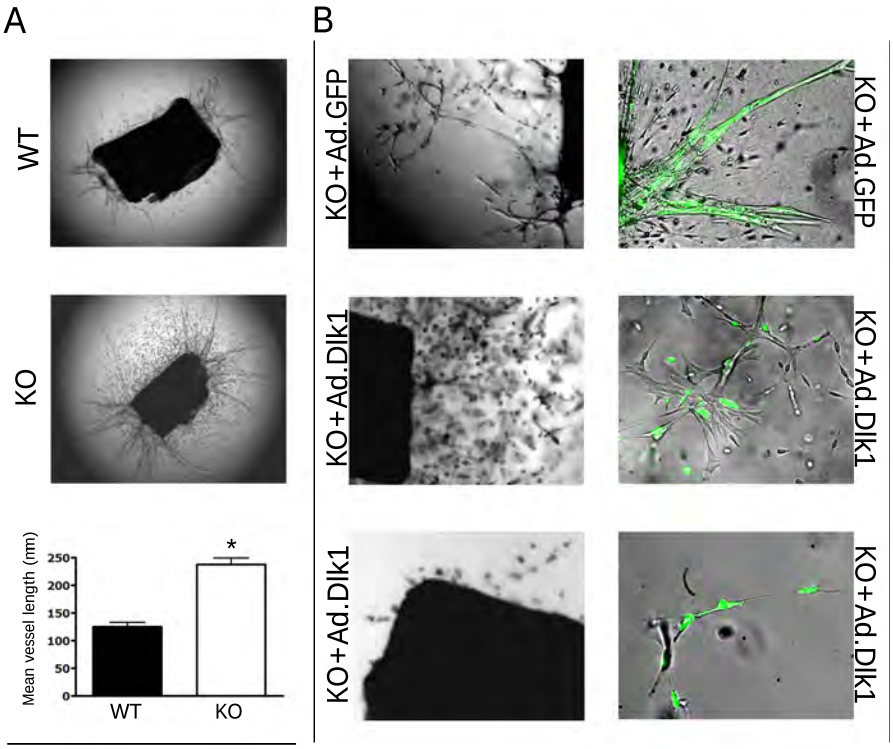
A
B
WT
KO
Mean vessel length (nm)
250
200
150
100
50
0
*
WT
KO
KO+Ad.GFP
KO+Ad.GFP
KO+Ad.Dlk1
KO+Ad.Dlk1
KO+Ad.Dlk1
KO+Ad.Dlk1

Fig 2

A

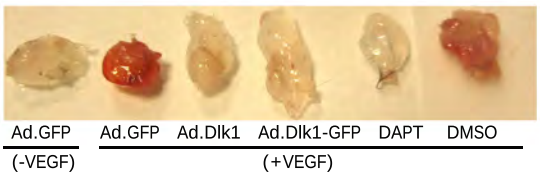
Ad.GFP
Ad.GFP
Ad.Dlk1
Ad.Dlk1-GFP
DAPT
DMSO
(-VEGF)
(+VEGF)

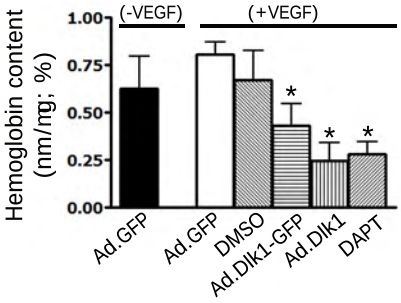
(-VEGF)
(+VEGF)
Hemoglobin content
(nm/mg; %)
1.00
0.75
0.50
0.25
0.00
*
*
*
Ad.GFP
Ad.GFP
DMSO
Ad.Dlk1-GFP
Ad.Dlk1
DAPT

B

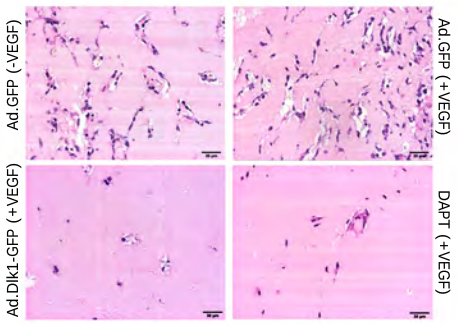
Ad.GFP (-VEGF)
Ad.GFP (+VEGF)
Ad.Dlk1-GFP (+VEGF)
DAPT (+VEGF)

C

Fig 3

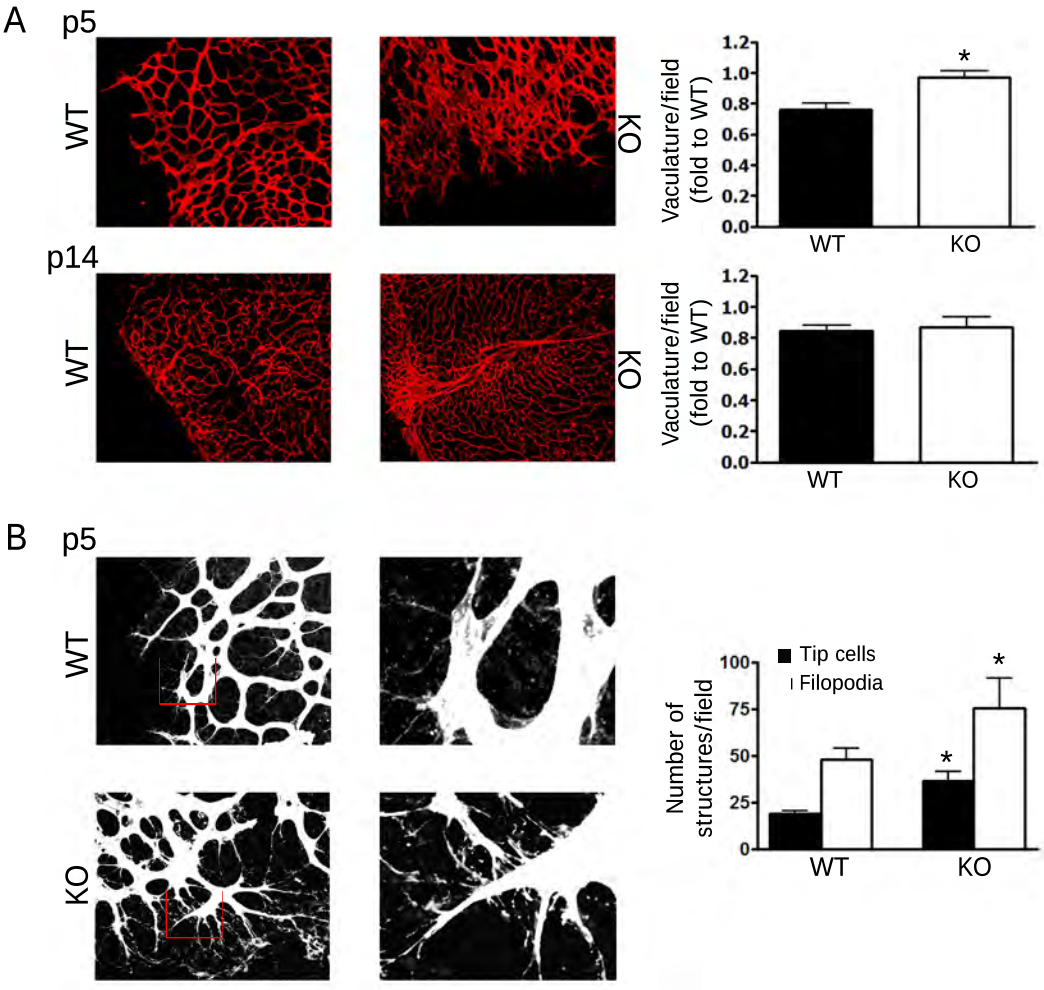
A
p5
WT
KO
p14
WT
KO
Vaculature/field (fold to WT)
1.2
1.0
0.8
0.6
0.4
0.2
0.0
*
WT
KO
Vaculature/field (fold to WT)
1.2
1.0
0.8
0.6
0.4
0.2
0.0
WT
KO
B
p5
WT
KO
Tip cells
Filopodia
Number of structures/field
100
75
50
25
0
*
*
WT
KO

Fig 4

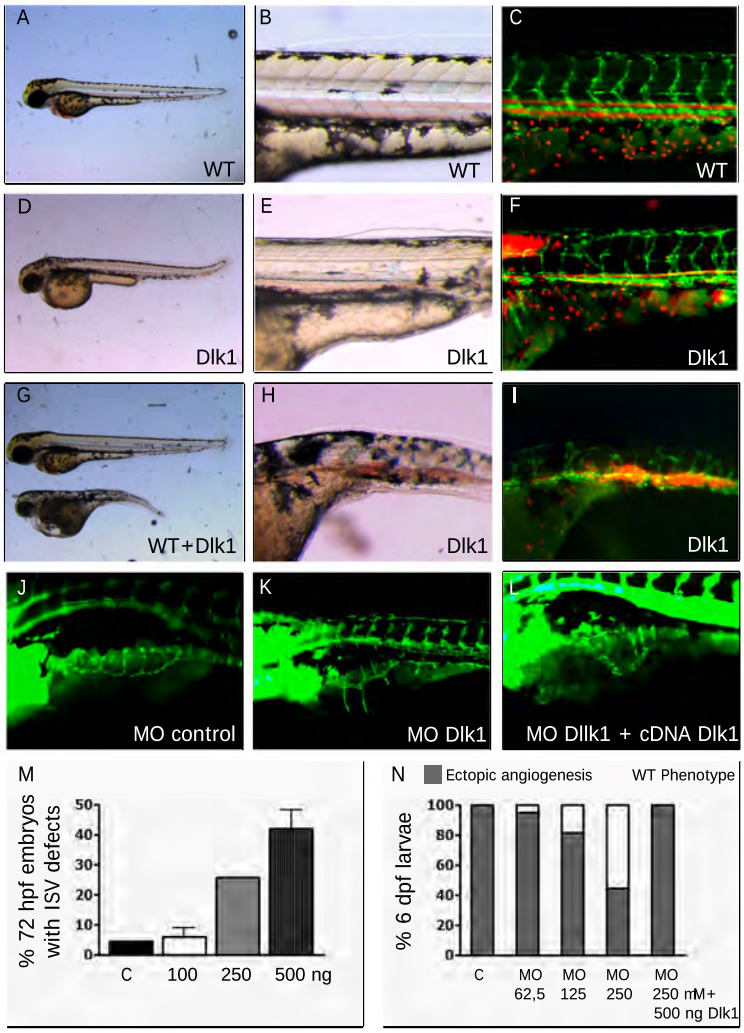
A
WT
B
WT
C
WT
D
Dlk1
E
Dlk1
F
Dlk1
G
WT+Dlk1
H
Dlk1
I
Dlk1
J
MO control
K
MO Dlk1
L
MO Dllk1 + cDNA Dlk1
M
% 72 hpf embryos with ISV defects
50
40
30
20
10
0
C
100
250
500 ng
N
Ectopic angiogenesis
WT Phenotype
% 6 dpf larvae
100
80
60
40
20
0
C
MO 62,5
MO 125
MO 250
MO 250 mM+ 500 ng Dlk1

Fig 5

Supporting online material

Adenoviruses

Adenoviruses encoding GFP, Dlk1-GFP or Dlk1-HA were obtained from Vector Biolabs. Adenoviruses were purified using the Adeno-X Maxi Purification Kit (Clontech) and titered using the Adeno-X Rapid Titer Kit (Clontech)

Cell lines, endothelial cells isolation and culture

Mouse 3T3-L1 cell line was routinely maintained in DMEM with 10% bovine calf serum and 1% penicillin-streptomycin (P/S). The 293A cell line was maintained in DMEM with 10% fetal bovine serum (FBS) for amplifying the adenoviruses. Bovine aortic endothelial cells (BAEC) and porcine aortic endothelial cells (PAEC) were cultured as described [S1, S2, S3]. For mouse lung endothelial cells (MLEC) isolation, lungs from 129 SVJ wild-type and Dlk1 null mice were excised, collagenase-digested, and further disaggregated to produce a single cell suspension. The mixed population obtained was first subjected to negative selection with anti FCsRII/III antibody (CD16/CD32) (BD™) and then to positive selection with anti ICAM-2 antibody (CD102) (BD™) and anti-IgG-coated magnetic beads (Invitrogen). MLECs were grown on a mixture of fibronectin (Sigma), type I collagen (Vitrogen 100) and 0.1% gelatine (Sigma) coated plates with DMEM + Ham´s F-12, 20% FBS, 1% P/S, 2 mM Glutamine and brain cow extract growth factor for endothelial cells (ECGF). For human umbilical vein endothelial cells (HUVEC) isolation, umbilical cords were digested with 0.1% collagenase at 37ºC for 20 minutes. Endothelial cells were collected and grown on 0.2% gelatin with Medium 199 + 20% FBS, 1% P/S and ECGF. Animals were handled as approved by the European and Spanish laws and regulations governing the use and protection of vertebrate mammals for scientific experimental purposes. Human umbilical cords were donated for scientific purposes only.

Western Blot Analysis

Cells were lysed in RIPA buffer with a Protease Inhibitor cocktail (Roche) and 1% SDS, then these lysates were sonicated and incubated at 4ºC for 30 minutes. Total

protein concentration was determined using BCA reagent (Pierce). Lysates were subjected to 10% SDS-PAGE electrophoresis and transferred to nitrocellulose membranes (Millipore). Membranes were blocked with TBS containing 5% BSA or milk for 1 h and probed with Dlk1 antibody (1:2500; Santa Cruz), anti-NICD (1:1000; Abcam), anti-Hey (1:1000; Santa Cruz), anti-Slug (1:500; Santa Cruz) and anti-Actin (1:10000; Sigma). Following incubation at 4ºC overnight, membranes were incubated with anti-rabbit or anti-mouse (Odyssey, 926-32211 and 926-32220, respectively) at room temperature for 1h. Detection was performed using the Li-Cor Odyssey Infrared Imaging System. The optical density of the protein bands was analyzed by Multi-Gauge V3.0.

RNA extraction and quantitative real-time PCR

Cell monolayers were washed with phosphate-buffered saline, total RNA was prepared with phenol-cloroform extraction. cDNA synthesis was undertaken using iScript cDNA Synthesis Kit (Biorad). Quantitative real-time PCR was performed using C1000 Thermal Cycler CFX96 Biorad. The endogenous genes were amplified by Sso Fast Eva Green Supermix (Biorad) using the appropriate primers (Supporting Table 1). The amount of each target gene relative to the housekeeping gene GAPDH for each sample was determined using the formula $2^{-\Delta Ct}$/the comparative threshold cycle (Ct) method.

Cell transfection and luciferase assay

Dlk1 plasmid was obtained from Origene (Human cDNA clone, SC127962). A hemaglutinin tag was added in order to detect the exogenous protein. The Hes-1 luciferase reporter construction, containing a 350 bp mouse promoter fragment of the Hes-1 gene inserted upstream of the luciferase gene in pGL2, has been reported elsewhere[S4] . Endothelial cell cultures at 60-70% confluence were co-transfected with Hes-1 luciferase reporter plus Renilla vector with lipofectamine (Invitrogen). After 24 h transfection, luciferase activity was determined using the Dual Luciferase Reporter Assay System (Promega) and expressed as fold induction relative to levels obtained with transfection of control plasmids.

Scratch assay

Endothelial cell monolayers were mechanically wounded and the rate of coverage of the denuded area was monitored by time-lapse microscopy for 24 hours using a Leica AF6000 LX microscopy coupled to a monochromatic Hamamatsu CCD C9100-02 camera.

Tube-like structure formation in vitro

The microcapillary-like formation assay was performed by using 96-well culture plates coated with 40 µl of Matrigel (BD Bioscience)[S5] diluted 1:1 in Medium 199 per well. After 30 min at 37ºC, porcine endothelial cells ($3x10^4$) in 0.1 ml of 10% FBS-DMEM or mouse lung endothelial cells ($3x10^4$) in D-MEM:F-12 (1:1) + 8% FBS + 2 mM Gln with or without VEGF (5 ng/ml) (R&D System) were seeded on the polymerized Matrigel and incubated at 37ºC for 5-6 hours. Angiotubes were stained with MTT (Sigma) for 30 minutes. Images of the capillary-like structures were taken at 2x magnification with a Nikon eclipse TE2000-U inverted-microscope coupled to a digital-sight DS-2Mv. Tube formation was quantified by using the Angioquant software and double-checked by eye-counted.

Aortic ring assay

Angiogenesis was studied by culturing rings of mouse aorta in three-dimensional gels as described[S6]. Thoracic aortas were removed from mice sacrificed by cervical dislocation and immediately transferred to a culture dish containing ice-cold phosphate buffered saline. The periaortic fibro-adipose tissue was carefully removed without damage the aortic wall. Pieces of aortas were immediately exposed or not to recombinant adenoviruses at $1x10^9$ or $5x10^9$ plaque-forming units/ml. After four hours of infection, one-millimeter long rings were embedded in Matrigel Basement Membrane Matrix Growth Factor Reduced (BD Biosciences) in 96-well plates. Each well contained 100 µl of MCDB131 supplemented with 2.5% mouse serum, 1% glutamine and 1% P/S. After 6 days of culture, explants were examined by microscopy. The vessel length per ring was quantified by ImageJ software.

Matrigel plug assay in vivo

Growth Factor Reduced Matrigel Matrix Phenol Red-free (500 µl) (BD, Bioscience), heparin (0.3 mg/ml) (Sigma), and VEGF (250 ng/ml), adenovirus, DAPT (10 mg/kg of body weight) or DMSO (0.01%), as appropriate (see fig. 3) were injected subcutaneously in the abdominal region of wild-type mice. Animals were euthanized after day 10 of implantation, plugs were dissected and hemoglobin was measured using the TMB method (Sigma). Hemoglobin content was normalized to plug weight. In another set of experiments plugs were removed for immunohistological examination. Paraformaldehyde-fixed plugs were embedded in paraffin and sectioned followed by staining with hematoxylin and eosin.

Retinal isolation and staining

P0-P14 pups were sacrificed and eyes enucleated and fixed O/N in 1% PFA at 4ºC. Then, retinas were dissected out and whole-mount stained with biotinylated *Griffonia simplicifolia* isolectin B4 (Sigma-Aldrich) followed by streptavidin, Alexa Fluor 647 conjugate (Invitrogen) as described[S7]. Images from 8-10 retinas per experimental group were acquired in a Nikon A1R confocal microscope, and quantification of tip cells, filopodia and vascular area was carried out with ImageJ software.

Cell viability and proliferation

Cell viability assay was assessed using the Cell Proliferation Kit II (XTT; Roche). Endothelial cells were seeded in 96-well plates at a density of 3000 cells per well. XTT turnover was measured at 0, 24, 48, 72 and 96 hours by adding XTT labeling mixture and incubation for 4 h at 37ºC to allow color development. Cell proliferation was assessed by BrdU incorporation into endothelial cells at 4, 8 and 24 hours. The incorporated BrdU was detected by anti-BrdU (1:100; Abcam) followed by anti-rat (1:200; Alexa 488) antibody. Images were taken with a Nikon eclipse TE2000-U inverted-microscope coupled to a digital-sight DS-2Mv (40x and 60x magnification).

Zebrafish experiments

Zebrafish (*Danio rerio*) were maintained and raised under standard conditions at 28°C. Transgenic *Tg(fli1:EGFP)* and *Tg(gata1:dsRed)* embryos were used to track endothelial cell populations and blood flow. Tg*(fli1:EGFP); (gata1:dsRed)* were generated by standard crossing of individual lines. A plasmid encoding the human Dlk1 cDNA was injected at different concentrations in one-cell stage embryos. The same plasmid without the human Dlk1 cDNA was used as a control. Embryos were allowed to develop and pictures were taken at 72 hours post-fertilization (hpf) using a dissection scope equipped with epifluorescence (MZF16FA, Leica) and a digital camera (DFC310FX, Leica). Anti-sense morpholinos (MO) (5´-CCAAAACCTCACAGAAGCTCGTCAT-3´) (Gene-Tools, OR, USA) were designed to target the initiation codon (ATG) of the zebrafish *Dlk1* gene (NCBI Reference Sequence: XM_001921677.1). A random sequence MO was used as a control. Both constructions were injected at 62,5uM, 125 uM and 250 uM in one or two-cell stage embryos that were allowed to develop until 6 days post-fecundation (dpf) when pictures were taken. For the rescue experiment, Dlk1 morpholino at 250 uM and 500 pg of plasmid encoding the human Dlk1 were co-injected in one-cell embryos and pictures were taken at 6 dpf. In each experiment, up to 100 embryos per condition were analyzed.

Statistical analysis

All data are expressed as mean ± standard error of the mean (SEM) for n experiments. Comparisons were evaluated by Student´s t-test for unpaired data or one-way analysis of variance when parametric tests were possible or by non-parametric tests, as appropriate.

Supporting Table 1

Primer	**Sequence**
Dlk For Bovine	5´AGTGCCCATGGAGCTGAATG3´
Dlk For Mouse, Human, Scrambled	5´AGCACCTATGGGGCTGAATG3´
Dlk Rev Bovine	5´CCGGATGTCTAGGTCACAGAG3´
Dlk Rev Mouse	5´CCGAACGTCTATTTCGCAGAA3´
Dlk Rev Human, Scrambled	5´CCGAACATCTCTATCACAGAG3´
GAPDH For	5´GCCTGGTCACCAGGGCTGC3´
GAPDH Rev	5´CTCGCTCCTGGAAGATGGTGATGG3´
m Hey For	5´CACGCCACTATGCTCAATGT3´
m Hey Rev	5´TCTCCCTTCACCTCACTGCT3´
m Snail For	5´TCTGAAGATGCACATCCGAAGCCA3´
m Snail Rev	5´AGGAGAATGGCTTCTCACCAGTGT3´
Slug For	5´AGATGCACATTCGAACCCAC3´
Slug Rev	5´GTCTGCAGATGAGCCCTCAG3´

List of supplementary references

S1. L. A. Timmerman *et al.*, *Genes Dev* **18**, 99 (2004).

S2. S. Lamas, T. Michel, B. M. Brenner, P. A. Marsden, *Am J Physiol* **261**, C634 (1991).

S3. S. Lopez-Ongil, M. Saura, D. Rodriguez-Puyol, M. Rodriguez-Puyol, S. Lamas, *Am J Physiol* **271**, H1072 1996).

S4. S. Jarriault *et al.*, *Nature* **377**, 355 (1995).

S5. M. Isaji, H. Miyata, Y. Ajisawa, Y. Takehana, N. Yoshimura, *Br J Pharmacol* **122**, 1061 (1997).

S6. N. A. Mikirova, J. J. Casciari, N. H. Riordan, *J Angiogenes Res* **2**, 2 (2010)

S7. M. E. Pitulescu, I. Schmidt, R. Benedito, R. H. Adams, *Nat Protoc* **5**, 1518 (2010).

Supplementary Figure legends

Table 1. Dlk1 is detected in adult endothelial cells. PCR cycle number (Ct) average of three independent preparations from bovine, murine, porcine and human endothelial cells showing Dlk1 expression at low levels compared to 3T3 pre-adipocytes.

Fig. S1. Dlk1 is expressed in adult endothelial cells from several species. Dlk1 dimmer is identified in non boiled lysates from mouse, human, pig and cow by a specific antibody. Samples were assayed from two independent preparations. Actin is used as a loading control.

Fig. S2. Dlk1 overexpression inhibits *in vitro* angiogenesis. Microvessel-like structures formed by porcine endothelial cells under basal conditions or by cells transfected with a control vector, pCMV6, or a Dlk1 plasmid in the absence or presence of VEGF. Quantification of the number of tube-like structures from three independent preparations per group assayed per duplicate. Bars represent mean $\pm$ SEM; *, # P>0.05

Fig. S3. Dlk1 regulates motility of vascular endothelial cell. Endothelial cell monolayers were mechanically wounded and rate and extent of endothelial cell migration into the denuded area were monitored by time-lapse microscopy for 24 hours.

(**A**) Representative images from porcine aortic endothelial cells under basal conditions, expressing a control vector, pCMV6, overexpressing Dlk1 or treated with DAPT, at time zero and at the time of the control closure. Red lines mark the edge of the "wound". (**B**) Representative pictures of lung endothelial cells from wild-type and Dlk1-KO mice. (**C**) Quantitative analyses represent percentage of the wound area at closure time, respectively (mean ± SEM of n=3 independent preparations assayed per triplicate; *P>0.05).

Fig. S4. Endothelial cell proliferation is increased in Dlk1 KO mice. (**A**) Quantitative analysis showing a higher viability in lung endothelial cells from KO mice compared to wild-type. Error bars represent SEM from at least three independent preparations (*P>0.05). (**B**) Quantification of BrdU-positive cells showing increased cell proliferation in Dlk1 KO mice. Representative images from BrdU (green) and DAPI (blue)-stained cells from wild-type and KO mice at 24 hours.

Fig. S5. Retinal hypervascularization in the Dlk1 KO developing vasculature. Whole-mount immunofluorescence for isolectin B4 in the p5 and p14 KO pups showing areas of a dense, hyperfused plexus in the retinal endothelium. Quantification of retina coverage by vessels at the affected areas vs non-affected in the same retina from KO mice. Values represent mean ± SEM from10 mice per group (*P>0.05)

Fig. S6. Notch signaling is decreased in endothelial cells overexpressing Dlk1. (**A**) Quantification of Notch signaling in bovine endothelial cells measured by Hes-1 activity. Dlk1 co-transfection decreases Notch activity in a dose-dependent fashion. (**B**) cDNA Dlk1 (0.25 μg) decreases Hes-1 activity to a similar extent than 0.5 μM of the gamma secretase inhibitor, DAPT. Bars represent mean ± SEM of three independent experiments assayed per triplicate (*P>0.05). Blot showing Dlk1-HA plasmid transfection.

Fig. S7. Notch signaling pathway is upregulated in Dlk1 KO mice. (**A**) Representative western blots from Notch intracellular domain (upper panel) and Hey1 (lower panel) showing protein upregulation in lung endothelial cells from KO mice. Quantification of four different mouse preparations per group by densitometry and qRT-PCR (mean ± SEM; *P>0.05). (**B**) Representative western blot from Slug protein. Quantitative qRT-PCR and densitometric analysis showing Slug and Snail are enhanced in Dlk1 KO mice.

Fig. S8. Notch intracellular overexpression enhances *in vitro* angiogenesis. Representative images from porcine endothelial cells transfected with a NICD plasmid from 0.5 to 6 μg (C-F) showing an increase in the capillary network formation compared to basal (A). Inhibition of the γ-gamma secretasa by 0.5 μM DAPT abolishes angiogenesis (B). Quantification of Hes-1 luciferase activity on cells co-transfected with NICD (1.5 μg) (upper graph) or treated with DAPT (lower graph). Bars represent mean ± SEM of three independent samples assayed per duplicate; *P>0.05

Fig. S9. Dlk1 overexpression does not affect capillary network formation in a stable NICD expressing cell line. Porcine endothelial cells overexpressing NICD transfected with a Dlk1 plasmid reflects a similar endothelial network than cells under basal conditions or cells transfected with a control plasmid, pCMV6. Quantitative analyses represent number of tube-like structures (upper graph) and Hes-1 luciferase activity on cells expressing pCMV6 or Dlk1 untreated or treated with DAPT (lower graph). Bars represent mean ± SEM of three independent experiments assayed per duplicate.

Fig. S10.

	Ct
BAEC	28.8 + 0.4
MLEC	33.1 + 0.5
PAEC	29.4 + 2.2
HUVEC	29.5 + 1.7
3T3-L1	17.4 + 0.5

Table 1

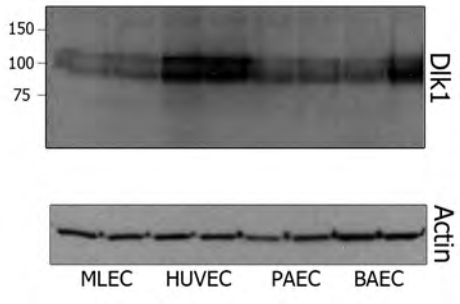

Fig S1

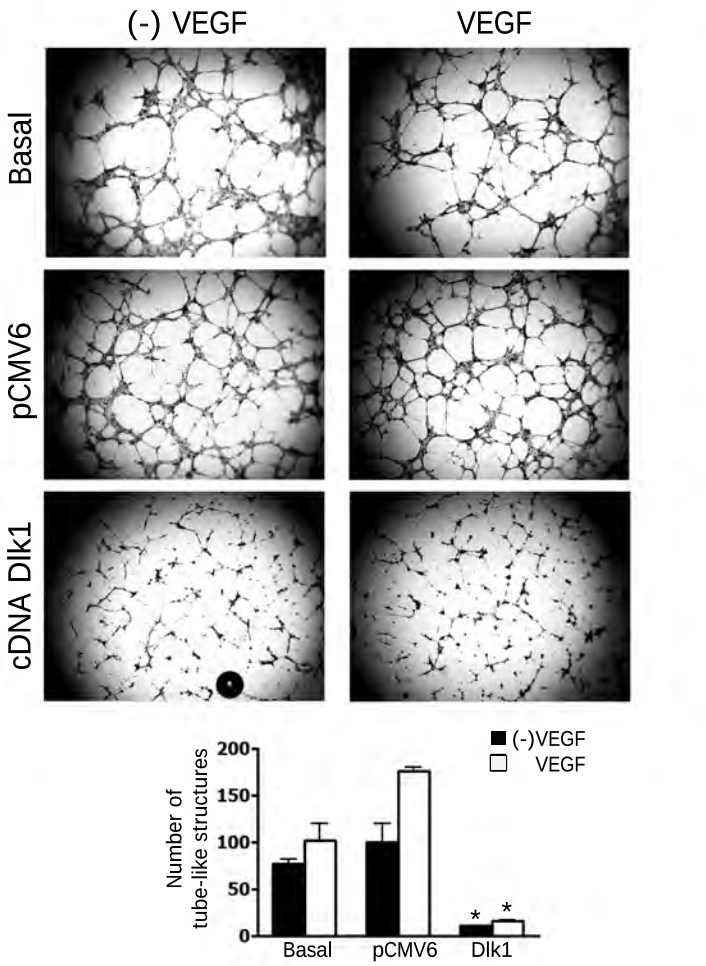
(-) VEGF
VEGF
Basal
pCMV6
cDNA Dlk1
(-)VEGF
VEGF
Number of tube-like structures
200
150
100
50
0
*
*
Basal
pCMV6
Dlk1

Fig S2

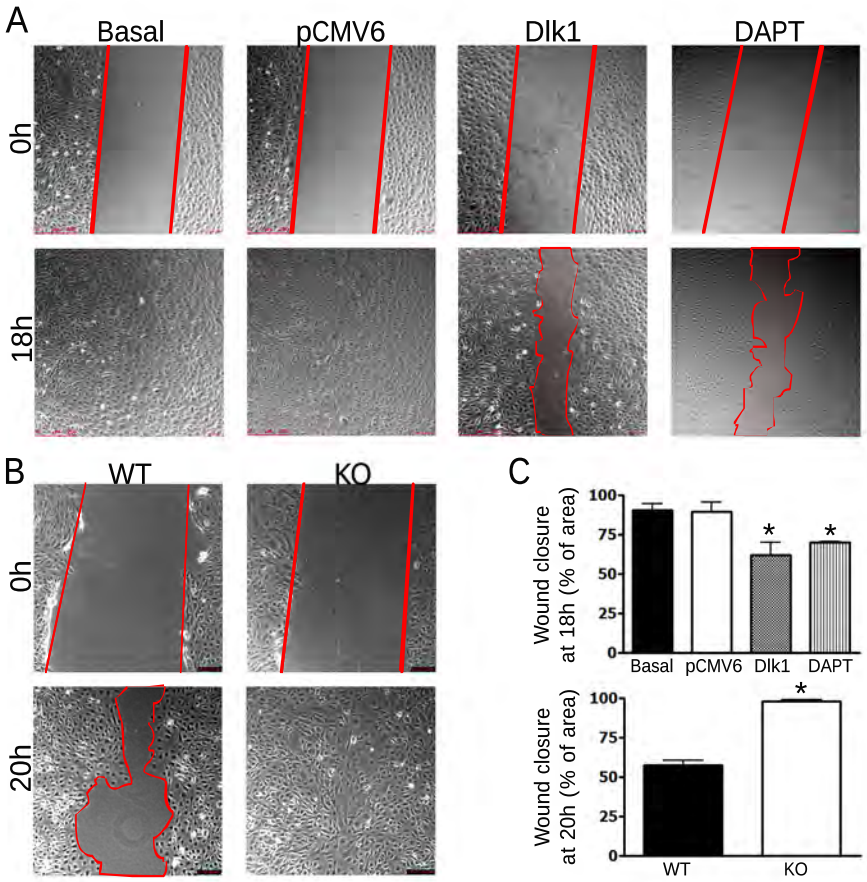
A
Basal
pCMV6
Dlk1
DAPT
0h
18h
B
WT
KO
0h
20h
C
Wound closure at 18h (% of area)
100
75
50
25
0
Basal
pCMV6
Dlk1
DAPT
*
*
Wound closure at 20h (% of area)
100
75
50
25
0
WT
KO
*

Fig S3

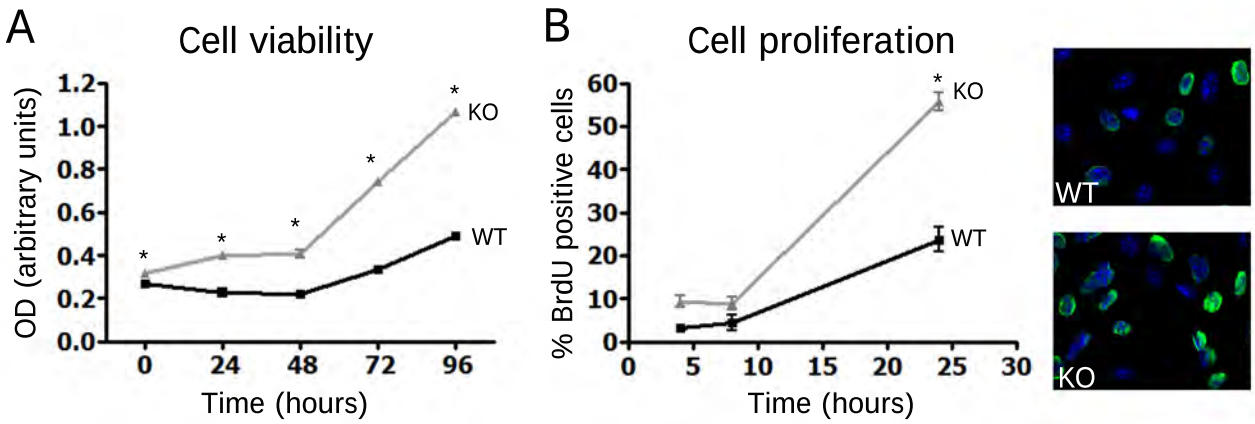
A
Cell viability
OD (arbitrary units)
1.2
1.0
0.8
0.6
0.4
0.2
0.0
0
24
48
72
96
Time (hours)
KO
WT
*
B
Cell proliferation
% BrdU positive cells
60
50
40
30
20
10
0
0
5
10
15
20
25
30
Time (hours)
KO
WT
WT
KO

Fig S4

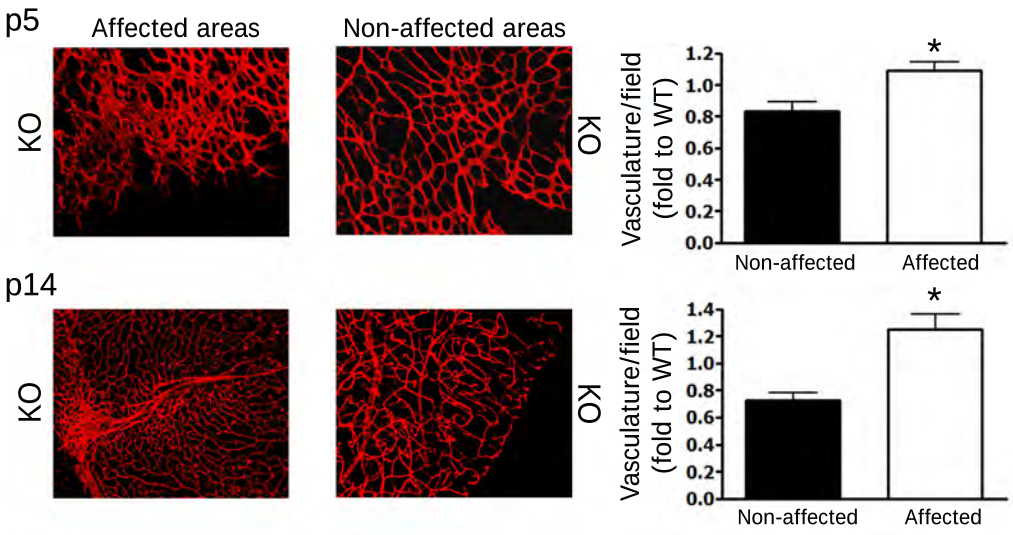
p5
Affected areas
Non-affected areas
KO
KO
Vasculature/field (fold to WT)
1.2
1.0
0.8
0.6
0.4
0.2
0.0
*
Non-affected
Affected
p14
KO
KO
Vasculature/field (fold to WT)
1.4
1.2
1.0
0.8
0.6
0.4
0.2
0.0
*
Non-affected
Affected

Fig S5

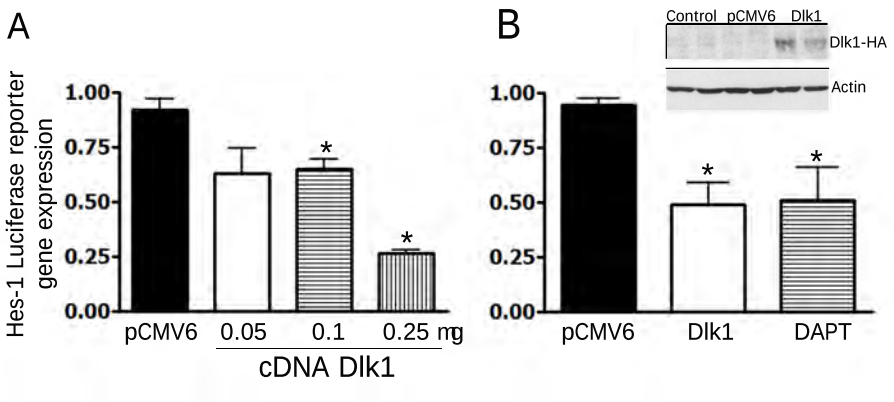
A
Hes-1 Luciferase reporter gene expression
1.00
0.75
0.50
0.25
0.00
*
*
pCMV6
0.05
0.1
0.25 mg
cDNA Dlk1
B
Control
pCMV6
Dlk1
Dlk1-HA
Actin
1.00
0.75
0.50
0.25
0.00
*
*
pCMV6
Dlk1
DAPT

Fig S6

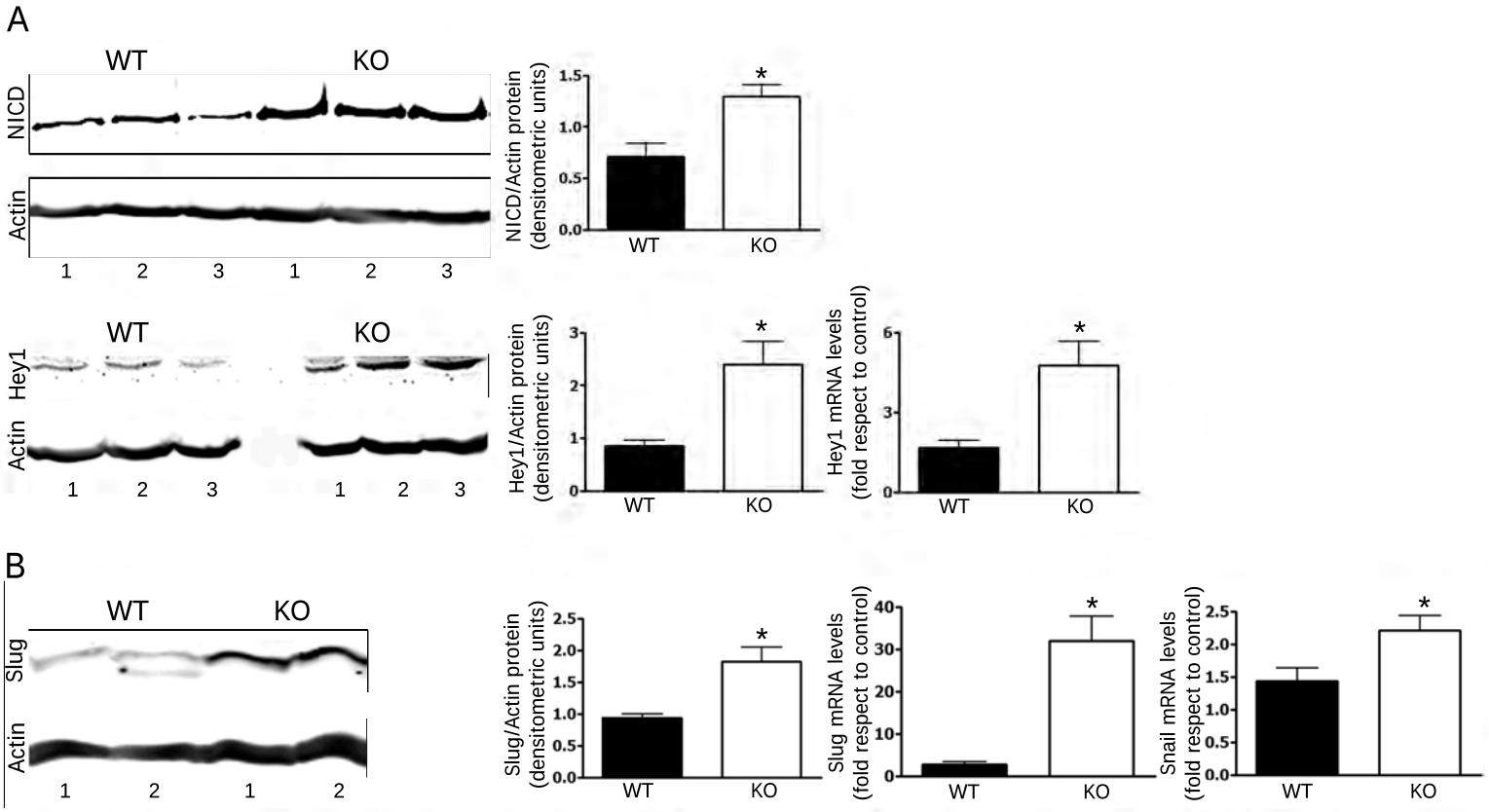
A
WT
KO
NICD
Actin
1 2 3 1 2 3
NICD/Actin protein (densitometric units)
WT
KO
Hey1
Hey1/Actin protein (densitometric units)
Hey1 mRNA levels (fold respect to control)
B
Slug
Slug/Actin protein (densitometric units)
Slug mRNA levels (fold respect to control)
Snail mRNA levels (fold respect to control)

Fig S7

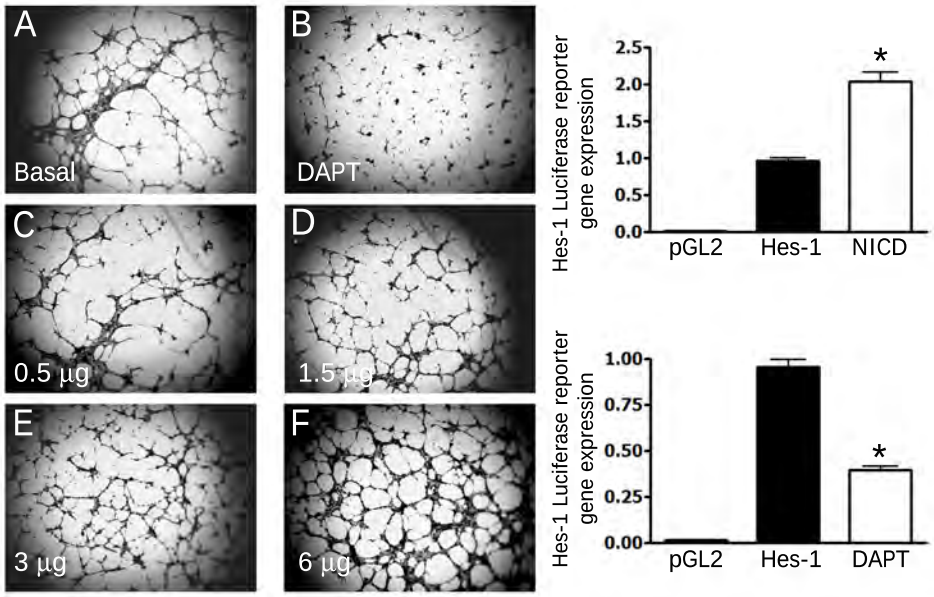
A
Basal
B
DAPT
C
0.5 µg
D
1.5 µg
E
3 µg
F
6 µg
Hes-1 Luciferase reporter gene expression
2.5
2.0
1.5
1.0
0.5
0.0
*
pGL2
Hes-1
NICD
Hes-1 Luciferase reporter gene expression
1.00
0.75
0.50
0.25
0.00
*
pGL2
Hes-1
DAPT

Fig S8

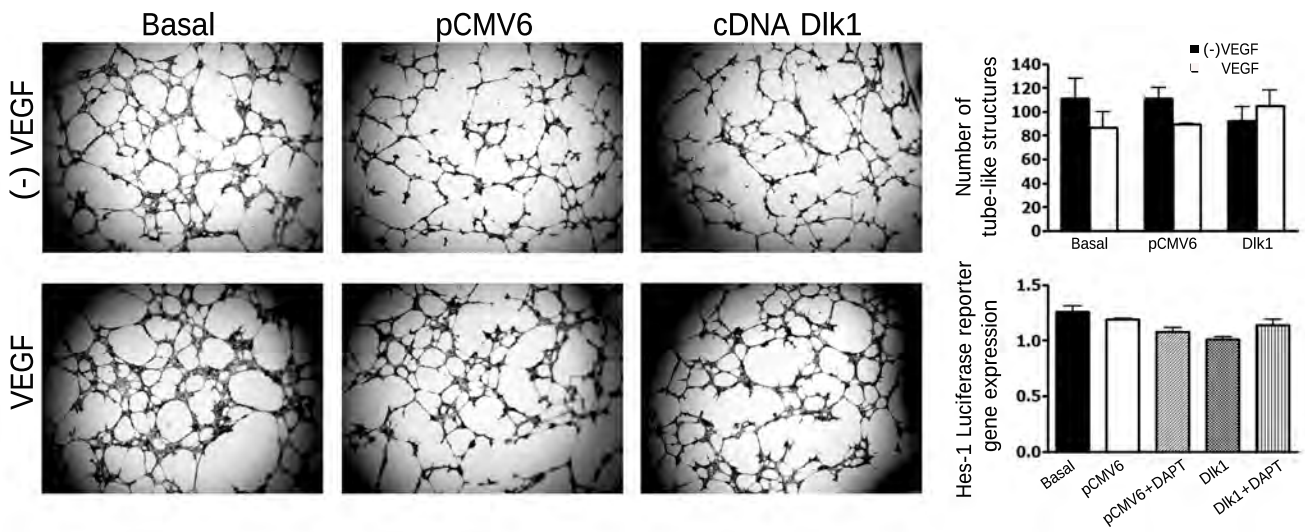
Basal
pCMV6
cDNA Dlk1
(-) VEGF
VEGF
Number of tube-like structures
(-)VEGF
VEGF
140
120
100
80
60
40
20
0
Basal
pCMV6
Dlk1
Hes-1 Luciferase reporter gene expression
1.5
1.0
0.5
0.0
Basal
pCMV6
pCMV6+DAPT
Dlk1
Dlk1+DAPT

Fig S9